Stomatal dynamics: a modeling study revisiting miscellaneous experimental phenomena

Xue Cong[a], Sien Li[b,c], Dan Hu[a,*]

[a]*School of Mathematical Sciences, Institute of Natural Sciences, and MOE-LSC, Shanghai Jiao Tong University, Shanghai, 200240, China*
[b]*Center for Agricultural Water Research in China, Agricultural University, Beijing 100083, China*
[c]*Shiyanghe Experimental Station for Improving Water Use Efficiency in Agriculture, Ministry of Agriculture and Rural Affairs, Wuwei 733000, China*

Abstract

Stomata are the key nodes linking photosynthesis and transpiration. By regulating the opening degree of stomata, plants successively achieve the balance between water loss and carbon dioxide acquisition. The dynamic behavior of stomata is an important cornerstone of plant adaptability. Though there have been miscellaneous experimental results on stomata and their constituent cells, the guard cells and the subsidiary cells, current theory of stomata regulation is far from clear and unified. In this work, we develop an integrated model to describe the stomatal dynamics of seed plants based on existing experimental results. The model includes three parts: 1) a passive mechanical model of the stomatal aperture as a bivariate function of the guard-cell and the subsidiary-cell turgor pressures; 2) an active regulation model with a targeted ion-content in guard cells as a function of their water potential; and 3) a dynamical model for the movement of potassium ions and water content. Our model has been used to reproduce different experimental phenomena semi and stomatal responses to environment conditions.

Keywords: stomata dynamics, turgor pressure, potassium flux, water potential, aperture

1. Introduction

The importance of stomatal behavior has been increasingly recognized in many fields including agricultural and food security (Macarisin et al., 2010), plant ecology (Brodribb and McAdam, 2014; Brodribb et al., 2016), environmental science (Hetherington and Woodward, 2003), and climate science (Hetherington and Woodward, 2003). The climate change has led to rapid shifts

*I am corresponding author.
Email addresses: congxue18@sjtu.edu.cn (Xue Cong), lisien@cau.edu.cn (Sien Li), hudan80@sjtu.edu.cn (Dan Hu)

in plant distribution (Kelly, 2008). In return, under the changing temperature and water availability, the distribution shifts and stomatal responses of plants play a key role in regulating the climate and water cycle (Hetherington and Woodward, 2003). An in-depth understanding of stomatal behavior is helpful for us to face the threat of global warming and water-resources redistribution (Hetherington and Woodward, 2003).

A stoma is a tiny opening on the epidermis of plants enclosed by a pair of bean-shaped (or dumbbell-shaped in grasses) guard cells (Steudle et al., 1977; Zimmermann and Schulze, 1980). Stomata of seed plants are present mostly on the lower epidermis of leaves. As a response to light, humidity, soil drought, and other factors, the turgidity of guard cells (and their surrounding cells) determines the aperture of the stomata, which is manifested as the opening and closing of stomata (PETER et al., 1978; Macrobbie and Lettau, 1980; Mott et al., 1997; Blatt, 2000; Shope and Mott, 2008; Inoue and Kinoshita, 2017; Buckley, 2019).

Stomata play as the key nodes connecting transpiration and photosynthesis of plants (Katul et al., 2010). When the stomata open, water in the leaf evaporates into the air; meanwhile, as an important element of photosynthesis, carbon-dioxide diffuses into the leaf through the stomata. The exchanging rate of water and carbon-dioxide is largely dependent on the stomatal aperture. By accurately regulating the aperture of stomata, plants successfully achieve the balance between water loss and carbon dioxide acquisition (Kollist et al., 2014; Lawson and Blatt, 2014). Such a balance becomes extremely important when water availability is limited.

There have been many models for stomatal conductance (Damour et al., 2010; Buckley and Mott, 2013; Dow et al., 2014; Miner et al., 2017), which is introduced to evaluate the transpiration rate. Nevertheless, researchers still encounter difficulties in real applications to predict transpiration rate with such models, because stomatal conductance is easily susceptible to many environmental conditions, such as light intensity (Sack and Holbrook, 2006), water availability (Martin Venturas D. and Hacke, 2017), atmospheric vapour pressure (Mott et al., 1997), carbon-dioxide concentration (Mott et al., 1993; Katul et al., 2010), temperature (Mott and Buckley, 2000; Rockwell et al., 2014), and wind speed (Shahraeeni et al., 2012). From this point of view, it is important to develop a physical model that naturally include the influences of these environmental factors.

Roughly speaking, environmental factors can either directly affect the guard-cell turgor by changing the mesophyll water potential or can induce active regulation of the guard-cell turgor by changing the osmotic pressure in guard cells (Macrobbie and Lettau, 1980; Blatt, 2000; Buckley, 2019). With these

responses, plants successfully achieve the balance between the availability and loss of water and the supply and demanding of carbon-dioxide.

The shape, size, and density of stomata vary greatly among different species (Franks and Farquhar, 2007). Such differences are believed to be an important part of the adaptability to the environment of different species (Katelyn et al., 2018; Gray et al., 2020). The stomatal complex is also known to vary widely across plant species (Franks and Farquhar, 2007; Brodribb and McAdam, 2011). The stomata of non-seed plants such as ferns lack subsidiary cells (Franks and Farquhar, 2007; Brodribb and McAdam, 2011). On the contrary, most of the guard cells of seed plants are surrounded by subsidiary cells, which are accessory cells providing support for the functioning of stomata (Katelyn et al., 2018; Gray et al., 2020). Stomata of different plant species may have varied number of subsidiary cells.

Experimental and modeling studies have aimed to quantitatively describe the relation between the stomatal aperture and the turgors of guard cells and subsidiary cells. The turgor pressure of guard cells provide the mechanical support to open the stomatal pores (PETER et al., 1978). A strong mechanical interaction between guard cells and their adjacent subsidiary cells are observed by cryo-electron microscopy (Franks and Farquhar, 2007). Since there is no subsidiary cells in ferns and lycophytes, their stomatal aperture are mediated only by the turgor pressure of guard cells (Franks and Farquhar, 2007; Brodribb and McAdam, 2011). For seed plants, the maximal stomatal aperture is obtained when epidermal (subsidiary) cells were at about incipient plasmolysis (Glinka, 1971; Franks et al., 1998; Franks and Farquhar, 2007). In general, increase of the epidermal (subsidiary) turgor pressure leads to decrease of stomatal aperture (Glinka, 1971; Cooke et al., 1976; Meidner and Bannister, 1979). These observations suggest the importance of the subsidiary-cell turgor in determining stomatal aperture for seed plants. In fact, the stomatal aperture is found to be more sensitive to the subsidiary-cell turgor than guard-cell turgor (Cooke et al., 1976). An antagonism ratio was used to characterize such a difference in sensitivity (Cooke et al., 1976; Meidner and Bannister, 1979). Based on the development of experimental technology in measuring turgor pressure (Franks, 1995), stomatal apertures are coordinated with successively changing guard-cell turgor under certain epidermis turgor (Franks et al., 1998). These studies provide an increasingly clear picture on the mechanical response of the stomatal complex.

The turgor pressure of guard cells and subsidiary cells is mainly determined by their water potential and solution concentration (osmotic pressure). Movement of the potassium ions can significantly change the osmotic pressure in the stomata complex. The potassium concentration in guard cells is observed

to change in an opposite direction with that in subsidiary cells (Macrobbie and Lettau, 1980; Blatt, 2000; Hedrich, 2005; Franks and Farquhar, 2007; Andres et al., 2014). As a result, plump (collapsed) guard cells and collapsed (plump) subsidiary cells are observed at the fully open (close) state (Franks and Farquhar, 2007). These studies provide a microscopic understanding on the physical means of active regulation of guard-cell turgor and stomatal aperture.

The mesoscopic stomatal dynamics also attract wide interests. The "wrong-way" response (WWR) was observed in many seed plants (Mott et al., 1997; Mott and Buckley, 1998; Mott et al., 2008; Shope and Mott, 2008; Cardon et al., 1994; Buckley, 2016, 2019), which is a transient wrong-way movement (followed by a 'right-way' movement(Buckley, 2019)) of the stomatal aperture under sudden change of environmental conditions such as the air humidity. When the environmental conditions are fixed, the stomatal apertures can usually reach a steady state. However, under certain conditions, they can also oscillate periodically (Mott et al., 1993; Mott and Buckley, 2000; Mott and Peak, 2006; Marenco et al., 2006). As a collective behavior of the oscillatory dynamics, stomata patchiness are widely observed in different species, which means spatially heterogeneous but locally synchronized oscillation of the stomatal apertures in a single leaf blade (Mott et al., 1993; Mott and Buckley, 2000; Marenco et al., 2006).

The continuous studies on stomatal mechanics and behaviors have provided profound insights on the realization of stomatal functions. Nevertheless, there is still a lack of a unified and integrated theory to explain various phenomena of stomata. This is partly due to the diversity in the configuration of stomata complex. In this work, we ignore such differences and establish a unified functional model for the stomata dynamics. Our model includes three parts: 1) a passive mechanical model of the stomatal aperture as a bivariate function of the guard-cell turgor and the subsidiary-cell turgor; 2) an active regulation model with a targeted ion-content in guard cells corresponding to their water potential; and 3) a dynamical model for the movement of potassium ions and the exchange of water content between the stomata complex and the air environment.

Using our model with the parameters partly determined with existing experimental data, we semi-quantitatively explain miscellaneous experimental results of the stomata dynamics such as emergence of the wrong-way response and Glinka's experimental results on soaked leaves (Glinka, 1971). Consistent to experimental observations (Marenco et al., 2006; Mott and Peak, 2006), rich dynamical behaviors of stomata are observed in our model. These successes indicate the validity of our model. Furthermore, our model provides a bridge

between the microscopic regulation mechanisms and the mesoscopic stomatal function. Effects of environmental conditions can be naturally incorporated in our model.

2. Modeling Stomatal Dynamics of Seed Plants

As mentioned above, the stomatal aperture of seed plants are mediated by the guard-cell and subsidiary-cell turgors. Despite the variations in cell configuration and stomata size across plant species, we develop a two-element model to describe different stomatal responses of seed plants.

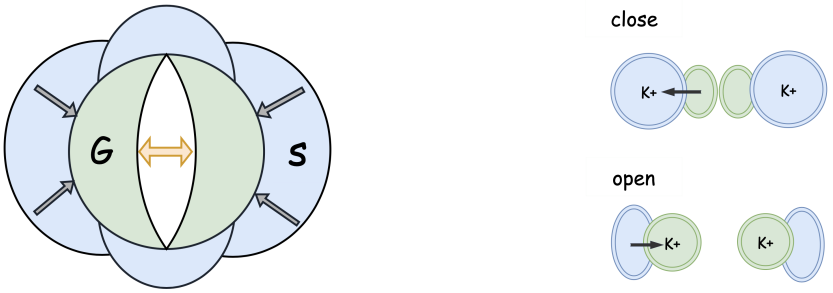

(a) Mechanical interaction (b) Ion transport

Figure 1: Interactions between the guard cells (light green) and the subsidiary cells (wathet blue). (a) The balance of the supporting force due to guard-cell turgor and the squeezing force due to subsidiary-cell turgor determines the stomatal aperture. (b) Active movements of potassium ions change the turgor pressure in the guard cells and subsidiary cells, leading to close (the upper panel) or open (the bottom panel) of the stoma.

As shown in Figure 1, our model mainly describes the interaction between the guard cells and the subsidiary cells of a stoma and their responses to environmental conditions. The turgor pressure of the guard cells provides the supporting force to open the stoma, whereas that of the subsidiary cells squeezes the guard cells from outside to close the stoma (see Figure 1 (a)). The competition of these two effects determines the stomatal aperture. Consequently, the stomatal aperture is determined by a bivariate function $a = a(P_g, P_s)$, where P_g and P_s are the guard-cell and subsidiary-cell turgor pressures, respectively.

Meanwhile, as a response to environmental changes, active regulation of the stomatal aperture is achieved by exchange of potassium ions between the guard cells and the subsidiary cells. The movement of potassium ions changes their osmotic pressure simultaneously. In our model, we assume that the regulation aims at an environment-determined target content (concentration) of potassium ions in guard cells. Two effects are included to describe the dynamical movement of the stomata: the movement of potassium ions between the guard cells and the subsidiary cells and the exchange of water content between the stomatal complex and the air in the substomatal cavity. In particular, as shown in Figure 1 (b), when potassium ions move from the subsidiary cells

to the guard cells, the guard-cells swell by absorbing water whereas the subsidiary cells shrink due to water loss. As a result, the turgor pressure increases in the guard cells and decreases in the subsidiary cells, which leads to opening of stomata. Similarly, the opposite movement of potassium ions leads to close of stomata.

2.1. The Passive Mechanical Model

Following previous studies (Cooke et al., 1976; Meidner and Bannister, 1979), we assume that the stomatal aperture is determined by the turgor pressures of the guard cells and the subsidiary cells, $a = a(P_g, P_s)$. In the work of Franks, Cowan, and Farquhar (Franks et al., 1998), the subsidiary-cell turgor pressure P_s is replaced by the epidermal turgor pressure P_e. We note that the turgor pressure in the subsidiary cells can differ from that in general epidermal cells, since the potassium content in subsidiary cells can change a lot during the regulation of guard cell turgor (Franks and Farquhar, 2007). We would also like to argue that the stomatal aperture should be dependent on P_s instead of P_e since only the subsidiary cells interact with the guard cells directly in seed plants. Another evidence to support our assumption is the lack of stomatal regulation in ferns and lycophytes, which have no subsidiary cells in their stomata.

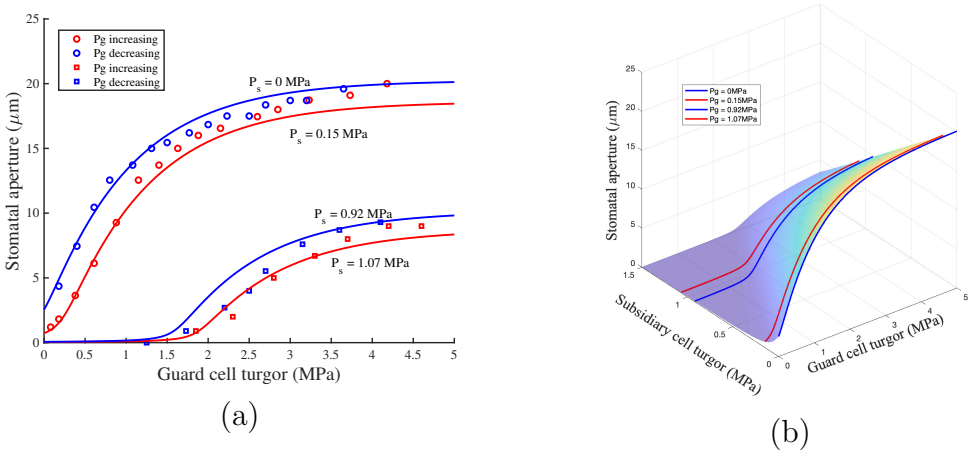

Figure 2: The relationship between guard-cell turgor and stomatal aperture under different subsidiary-cell turgor P_s. (a) Experimental data obtained in Ref. (Franks et al., 1998) and the fitting curves; (b) Illustration of the bivariate function $a = a(P_g, P_s)$.

Among all existing measurements, the work of Ref. (Franks et al., 1998) provides the most comprehensive and clear data for us to obtain a useful bivariate function $a = a(P_g, P_s)$, though they did not measure the subsidiary-cell turgor pressure. In their work, the stomatal aperture of *T. virginiana* is recorded for successively varying guard-cell turgor pressure (by injecting and sucking out silicon oil) under two different water potentials (Franks et al., 1998). As shown in Fig. 2 (a), the squares and the circles show the data

obtained under the water potential of -0.063MPa and -1.0MPa, respectively. The red squares and circles are obtained by increasing the guard-cell turgor, whereas the blue squares and circles are obtained by decreasing the guard-cell turgor.

Since the experiment is performed in a relatively short time compared to the regulation of stomata aperture, we assume that the ion content in the subsidiary cells does not change significantly during the experiment. This assumption means that the turgor pressure of the subsidiary cell in the experiment approximately maintains a constant. In the work of Ref. (Franks et al., 1998), the turgor pressure of epidermal cells are estimated to be 0.92MPa (squares) and 0.0MPa (circles), respectively. Before the experiment, the leaf is prepared in a dark environment and the stomata are fully closed. In this case, a large amount of potassium ions have moved from the guard cells to the subsidiary cells and the subsidiary cells have a relatively high turgor pressure. Comparing the ion concentration in the epidermal cells and the subsidiary cells (Macrobbie and Lettau, 1980), we roughly estimate that the turgor pressure is $0.10 \sim 0.20$MPa higher in the subsidiary cells than the epidermal cells when the stomata is closed.

In principle, the bivariate function $a(P_g, P_s)$ may differ among plant species. From the experimental data (Franks et al., 1998), we assume that the attainable maximum aperture is dependent on P_s. Making use of the concept of "antagonism ratio" defined in Ref. (Cooke et al., 1976), we fit the data in Ref. (Franks et al., 1998) by

$$a(P_g, P_s) = a_{\mathrm{m}}(P_s) \cdot f(w(P_g, P_s)), \tag{1}$$

where the attainable maximum aperture is fitted by $a_{\mathrm{m}}(P_s) = c_1 P_s^2 + c_2 P_s + c_3$, and $f(w)$ is the relative opening degree of the stomata

$$f(w) = 1 - \exp(-\frac{1}{2}(w + \sqrt{w^2 + k})),$$

where $w = w(P_g, P_s) = b_1 \cdot (P_g - A_r \cdot P_s) + b_2$ and A_r is the antagonism ratio (Cooke et al., 1976). The antagonism ratio refers to the ratio of the sensitivities of the stomatal aperture with respect to P_s and P_g, which is greater than 1 in general. The fitted parameters of the passive model are included in Table 1. We would like to point out these parameters could be specie dependent and more data are required to accurately determine these parameters for each specie.

A three-dimensional illustration of the bivariate function $a(P_g, P_s)$ is shown in Fig. 2 (b). Clearly, the stomatal aperture increases with the guard-cell turgor whereas decreases with the subsidiary-cell turgor. By fixing P_s at 0,

Parameter	b_1	b_2	k	A_r	c_1	c_2	c_3
Value	1.0	0.10	0.040	1.8	-5.16	-4.65	20.3
Unit	MPa^{-1}	–	–	–	$\mu\text{m/MPa}^2$	μm/MPa	μm

Table 1: Parameters of passive mechanical model.

0.15, 0.92 and 1.07MPa (which are slightly higher than the corresponding turgor pressure in epidermal cells), the curves are shown in both Fig. 2 (a) and (b). These curves fit well the experimental data for $P_E = 0$ and 0.92MPa in Ref (Franks et al., 1998), which suggests the validation of the bivariate function. In particular, as shown in Fig. 2 (a), for a same guard-cell turgor pressure, the measured aperture is smaller during the oil-injection process than that in the oil-suction process. This might be a consequence of potassium leaking of subsidiary cells during the experiment. Such a leaking leads to a slight decrement of the turgor pressure P_s, thus resulting in an increment of stomatal aperture.

3. Active-Control Model

Seed plants are capable of actively regulating their stomatal apertures. The regulation is mainly controlled by the movement of potassium ions between the guard cells and the subsidiary cells. Our active-control model consists of two parts. First, we assume that the active control of the ion movement is aiming at a target potassium ion content (concentration) in guard cells in response to its water potential. This relation between the potassium content and guard-cell water potential can also be observed at steady states. Second, we include the physical processes of ion movement and water exchange to develop a dynamical model for the active regulation.

3.1. The target relation between potassium content and guard-cell water potential

By controlling the water potential of the solution, Glinka studied the change of stomatal aperture of *vicia faba* leaf soaked in the solution (Glinka, 1971). Interestingly, as shown by the stars in Fig. 3 (a), the steady-state aperture of the stomata reaches the maximum at a water potential of $\Psi^* \approx -0.65$MPa. Further increase of the water potential, although implying more adequate water supply of the leaf, leads to decrease of the stomata aperture.

In our model, we assume that the regulation of stomatal aperture is achieved by actively controlling the ion movement between guard cells and subsidiary cells based on the guard-cell water potential Ψ_g. Obviously, a high potential Ψ_g indicates adequate water supply, thus potassium ions move from the subsidiary cells to the guard cells to open the stoma. As a result, the target ion

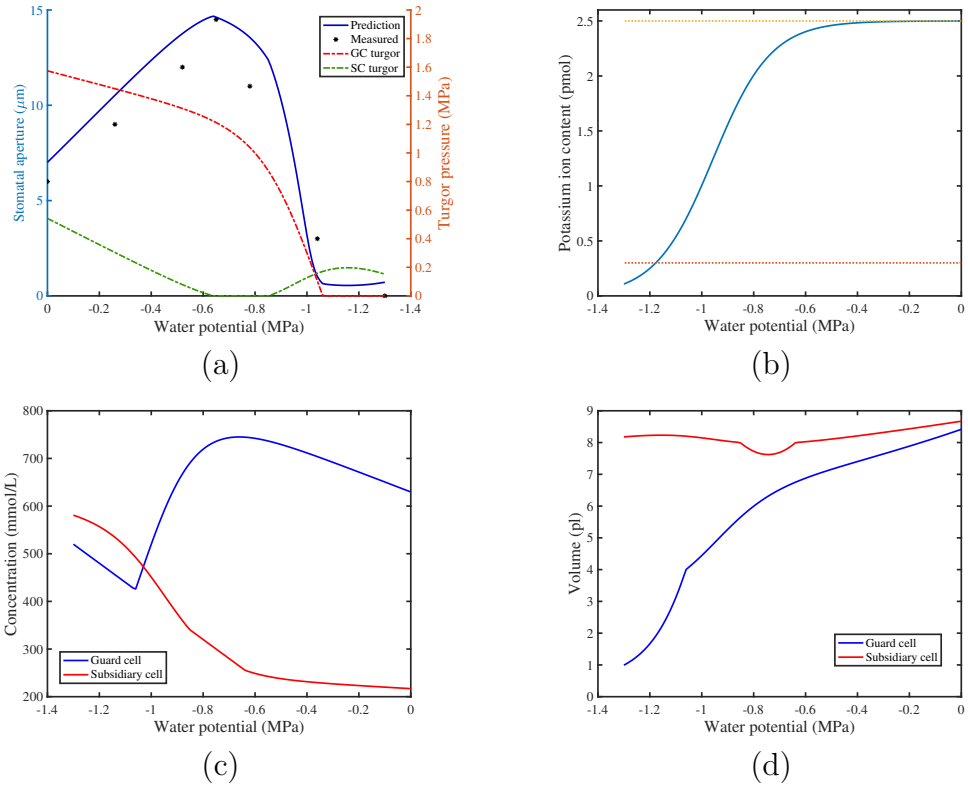

Figure 3: The target relation for active control of stomata aperture and prediction of Glinka's experimental result. (a) The steady-state stomatal aperture for different solution water potential. Stars: Glinka's measurements for leaves soaked in the solution; Blue solid line: model prediction; Red and green dashed lines: the model predicted guard-cell and subsidiary-cell turgors, respectively. (b) The target relation between potassium content and the water potential in the guard cells. (c-d) Model predicted potassium concentration and volume of the guard cell and the subsidiary cell.

content in the guard cell I_g^K should be a monotonic increasing function of Ψ_g, which is simply modeled by

$$I_g^K(\Psi_g) = \frac{I_m^K}{1 + \exp\left((-\Psi_g + \Psi_0) \cdot d_0\right)}, \tag{2}$$

where I_m^K is the maximum accessible potassium content in a guard cell, Ψ_0 is half-content reference potential, and d_0 indicates the sensitivity of the function. The parameters may also be specie-dependent. In particular, I_m^K is largely determined by the maximum volume of the guard cell, which can be different among species. Light intensity, carbon-dioxide concentration, and other factors may change the regulation and can be modeled by changing the parameters Ψ_0 and d_0.

With parameters shown in Table 3, a typical target relation between the potassium content and the guard-cell water potential is shown in Fig. 3 (b). The total potassium content is sensitive when the guard-cell water potential is between -1.3MPa and -0.6MPa. When the water potential is sufficiently high, the potassium content approximately reaches its maximum and becomes insensitive.

The total solute content in a guard cell I_g^0 is given by

$$I_g^0(\Psi_g) = 2I_g^K(\Psi_g) + I_g^{og}, \tag{3}$$

where $2I_g^K$ is the content of potassium ions and the anions (such as chloride ions), I_g^{og} indicates the total content of organic solutes and other ion contents. Using I_g^0 and the volume of the guard cells V_g, we are able to evaluate the total solute concentration and the osmotic pressure.

As discussed above, the change of potassium content in the guard cell is due to the exchange with the subsidiary cells. In other words, the subsidiary cell can be regarded as a potassium reservoir for the guard cell (Franks and Farquhar, 2007). Therefore, the solute content in the subsidiary cell can be evaluated by

$$I_s^0(\Psi_g) = I_s^m - 2\beta I_g^K(\Psi_g), \tag{4}$$

where I_s^m is the maximal solute content in a subsidiary cell and β represents the fraction of potassium ions absorbed by the subsidiary cells. Similarly, this solute content and the volume of the subsidiary cell V_s can also be used to evaluate the solute concentration and osmotic pressure in subsidiary cells.

At steady states, the water potentials in the guard cells and the subsidiary cells are given by

$$\Psi_i = -RT\frac{I_i^0(\Psi_g)}{V_i} + P_i, \tag{5}$$

where $i = s$ or g is used to represent the subsidiary cells and the guard cells,

respectively, R is the gas constant, T is the absolute temperature, and the turgor pressure P_i is given by (Raschke et al., 1988)

$$P_i = \begin{cases} \frac{\epsilon_i(V_i - V_{0i})}{V_i}, & \text{if } V_i > V_{0i}; \\ 0, & \text{if } V_i \leq V_{0i}, \end{cases} \tag{6}$$

where V_{0i} are the critical volumes for plasmolysis and ϵ_i are the volumetric elastic constants.

In principle, all the parameters in Eqs. (2)-(6) can be measured by experiments. Although a few of the parameters have not been directly measured, we are able to estimate the typical magnitude of the parameters for a model stoma using existing data. The volumes of typical guard cells and subsidiary cells (V_{0g} and V_{0s}) can be estimated from the experimental results in Ref. (Macrobbie and Lettau, 1980; PETER et al., 1978). The volumetric elastic modulus ϵ_g and ϵ_s are measured in Refs. (Zimmermann and Schulze, 1980). The potassium concentration in guard cells under various stomatal apertures is measured in the work of Macrobbie and Lettau (Macrobbie and Lettau, 1980), which can be used to estimate the parameters in Eq. (2), such as the maximum potassium content in a guard cell. Similar results are also reported in the work of Refs. (Hedrich, 2005; G et al., 1971). Based on these experimental results, the parameters used in this work are included in Table 3.

Parameter	Meaning	Value
I_m^K	Maximum content of K^+ in a guard cell	2.5pmol
Ψ_0	The sensitive water potential	0.70MPa
d_0	The slope parameter	$0.90(\text{MPa})^{-1}$
I_g^{og}	Minimum solute content in a guard cell	0.30pmol
I_s^m	Maximum solute content in a subsidiary cell	0.64pmol
β	Absorbing percentage of potassium ions by subsidiary cells	0.60
R	Gas constant	$8.314\text{J}/(\text{mol}\cdot\text{K})$
T	Kelvin temperature	300K
ϵ_g	Volumetric elastic modulus of guard cell	3.0MPa
ϵ_s	Volumetric elastic modulus of subsidiary cell	7.0MPa
V_{0g}	Incipient plasmolysis volume of guard cell	$4000\mu m^3$
V_{0s}	Incipient plasmolysis volume of subsidiary cell	$8000\mu m^3$

Table 2: Parameters for the target relation between ion contents and the guard-cell water potential.

Next, we use the model to explain Glinka's experimental results (Glinka, 1971). In Glinka's experiments, since the leaf is soaked in the solution, we

have $\Psi_g = \Psi_s = \Psi_0$, where Ψ_0 is the water potential of the solution. Using Eqs. (2)-(6), we can evaluate the volume and the turgor pressure of both types of cells. Then, using the passive mechanical model (1), we can evaluate the steady-state stomatal aperture under different water potentials of the solution.

The model-predicted results are shown in Fig. 3 (a). We can see that the stomatal aperture also reaches a maximum when the solution water potential is about $\Psi^* = -0.65$MPa. Further increase of the water potential really leads to reduction of stomatal aperture. In this case, as shown in Fig. 3 (a), there is a simultaneous increase of the turgor pressures in both the guard cells and the subsidiary cells. This leads to reduction of the stomatal aperture, because the stomatal aperture is more sensitive to the turgor change of the subsidiary cells than that of the guard cells.

As shown in Fig. 3 (a), the turgor pressure of the guard cells vanishes when the water potential is sufficiently low. Indeed, consistent to the experimental results (Glinka, 1971; Franks et al., 1998; Franks and Farquhar, 2007), the maximal stomatal aperture is obtained at about incipient plasmolysis of subsidiary cells. This is due to the active regulation process, which moves a large amount of potassium ions from the subsidiary cells to the guard cells. The concentration and cell volume of the two type of cells are shown in Fig. 3 (c) and (d). Using the the parameters in this work, the predicted change of the subsidiary-cell volume is not large. It requires more experimental verification or more experimental measurements to improve the parameters.

3.2. The dynamical regulation model of stomatal apertures

In order to describe the regulation dynamics of stomatal apertures, the active regulation of potassium flux is coupled with the evaporation of water from leaves to the air (transpiration). The transpiration process is illustrated in Fig. 4. The water potential in the substomatal air cavity affects the water evaporation of the guard cells and the subsidiary cells. Thus it dynamically changes the water potential in these cells and modulates the potassium flux and the stomata aperture; meanwhile, the stomatal aperture determines the stomatal resistance and regulate the water potential in the substomatal cavity. In other words, the regulation of stomatal aperture and the change of the water potential in the substomatal cavity are coupled with each other.

The modulation of potassium flux is modeled in a linear fashion,

$$\begin{cases} \dfrac{dI_g(t)}{dt} = -\dfrac{1}{\tau}(I_g - I_g^0(\Psi_g)), \\ \dfrac{dI_s(t)}{dt} = -\beta\dfrac{dI_g(t)}{dt}, \end{cases} \tag{7}$$

where I_g and I_s are the dynamical solute contents of the guard cell and the subsidiary cell, respectively, τ is the decay time, and $I_g^0(\Psi_g)$ is the target solute

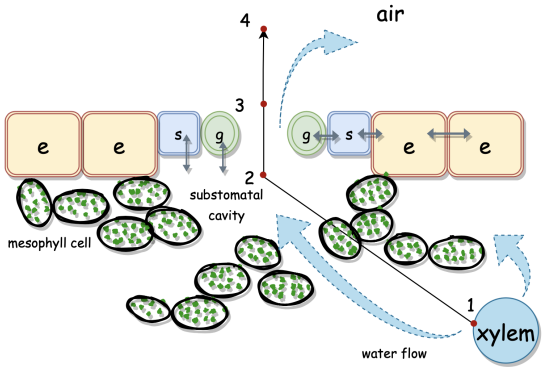

Figure 4: Illustration of the transpiration process and regulation of stomatal aperture. Cells in light green, blue, and yellow represent the guard cells, the subsidiary cells, and the epidermal cells, respectively. Water is exuded from the xylem, reaches the substomatal cavity through leaf cells and the air space in leaves, and diffuses into the air through the stoma.

content of the guard cell given by Eq. (3). Note that in the dynamical model, Ψ_g also evolves with time.

Since the solute content is already given by Eq. (7), we only need to find the volume of the two types of cells to evaluate their water potential utilizing Eq. (5) and (6). Evolution of the cell volumes of is determined by water exchanges between the cells and the substomatal cavity,

$$\begin{cases} \dfrac{dV_g(t)}{dt} = \dfrac{V_m A_{sg} P_m}{RT} \left((\Psi_s - \Psi_g) - n_1(\Psi_g - \Psi_2) \right), \\ \dfrac{dV_s(t)}{dt} = -\dfrac{V_m A_{sg} P_m}{RT} \left((\Psi_s - \Psi_g) + n_2(\Psi_s - \Psi_2) - n_3(\Psi_x - \Psi_s) \right), \end{cases} \tag{8}$$

where V_g, V_s are the dynamical volume of the guard cell and the subsidiary cell, respectively, V_m is the molar volume of liquid water, A_{sg} is the contact area between a guard cell and its neighboring subsidiary cell, P_m is the effective permeability of water molecules across two layers of cell membranes and cell walls, Ψ_2 and Ψ_x are the water potentials in the air cavity and the xylem, respectively, and n_1, n_2, and n_3 are nondimensional relative conductances taking into account the relative changes in permeability and area of the permeation surfaces. The parameters used in this work are included in Table. 3. In this work, we assume that Ψ_x is given as a fixed value, though in other applications it can be evaluated by the soil water potential, the conductance from plant root to leaf venation, and the total transpiration rate.

As discussed above, Ψ_g and Ψ_s can be evaluated using the solute contents and volumes based on Eq. (5) and (6). To close the system of Eqs. (7) and (8), we are left to determine the water potential in the substomatal cavity, Ψ_2. As illustrated in Fig. 4, three conductances have been employed in previous works (Damour et al., 2010; Buckley and Mott, 2013; Dow et al., 2014; Miner et al., 2017) to describe the transpiration process in leaves: the outside-xylem

conductance (K_{ox}, from the xylem to the substomatal cavity), the stomatal conductance (K_{st}, from the substomatal cavity to the outer surface of the stoma), and the boundary layer conductance (K_{bl}, from the outer surface of the stoma to the atmosphere). Usually, the conductances are defined for unit leaf area. Note that the conductances can be dependent on environmental conditions such as the temperature and wind speed. For convenience of use, we define the reciprocals of the conductances as the resistances, $R_i = \frac{V_m e_w}{(RT)^2}\frac{1}{K_i}$, where $i = ox, st$, and bl represents the index of the conductances, V_m is molar volume of liquid water, and e_w is the saturated water vapor pressure.

The outside-xylem conductance has been roughly discussed in a previous work (Scoffoni et al., 2017) based on experimental results. The stomatal resistance and the boundary layer resistance are evaluated in a modeling study (Vesala, 1998)

$$R_{st} = \frac{1}{C_{sto} \cdot D \cdot a}(\frac{1}{4} + \frac{L}{\pi a}), \tag{9}$$

$$R_{bl} = \frac{1}{4C_{sto} \cdot D \cdot a} + \frac{1}{\alpha D}\sqrt{\frac{\mu A_r}{\rho \cdot v_{wind}}}, \tag{10}$$

where a is the stomatal aperture, A_r is the effective leaf radius, v_{wind} is the wind speed, and the other parameters are included in Table. 3.

At steady states, the diffusion of water molecules is balanced. If the effects of spacial heterogeneity of temperature is negligible, the concentration (pressure) of water vapor in the air cavity is determined by the resistances discussed above. In real applications, the water potential is related with the vapor pressure by

$$\Psi_i = \frac{RT}{Vm} \ln \frac{e_i}{e_w}, \tag{11}$$

where e_i and e_w are the water-vapor pressure and the saturated vapor pressure, respectively, and the indices $i = x, 2$, and "air" represent the xylem end, the air cavity, and the atmosphere, respectively (as shown in Fig. 4). Water may exist in liquid form in the leaf. However, we can still define a corresponding vapor pressure using the water potential. Inside the leaf, the water potential is relatively high and Eq. (11) is approximately linear. As a result, the water-vapor pressure in the substomatal cavity can be linearly determined by (see appendix)

$$e_2 = (1 - \gamma(a, v_{wind})) \cdot e_x + \gamma(a, v_{wind}) \cdot e_{air}, \tag{12}$$

where $\gamma(a, v_{wind}) = \frac{R_{ox}}{R_{ox}+R_{st}+R_{bl}}$ depends on the stomatal aperture and wind speed. Other environmental conditions such as the temperature may also influence the parameters in Table. 3 and the value of γ.

Parameter	Meaning	Value
V_m	Molar volume of water	$18\text{cm}^3/\text{mol}$
A_{sg}	Contact area of a guard cell and a subsidiary cell	$300\mu\text{m}^2$
P_m	Permeability of water molecules	$10\mu\text{m/s}$
τ	Decay time	20min
n_1	Relative conductance	1
n_2	Relative conductance	1
n_3	Relative conductance	0.25
C_{sto}	Stoma density on the leaf	$90/\text{mm}^2$
D	Diffusion constant	$2.5 \times 10^{-5}\text{m}^2/\text{s}$
α	Empirical constant	0.941
μ	Dynamic viscosity	$1.7 \times 10^{-5}\text{N}\cdot\text{ s/m}^2$
ρ	Air density	1.29kg/m^3
v_{wind}	Wind speed	1.0m/s
A_r	Leaf radius	5cm
e_w	Saturated vapor pressure	$2.81kPa$

Table 3: Parameters for the transpiration process.

4. Numerical results of the dynamical model

According to our simulations, a few parameters in our model can change the dynamical behavior significantly, including the water potential at the end of the xylem Ψ_x, the outside-xylem conductance K_{ox}, and the water-vapor pressure in the air e_{air}. Other parameters, such as the wind speed v_{wind} and the leaf radius A_r, can also have a certain impact, but the dynamics are less sensitive to these parameters.

4.1. Stomatal dynamics

Consistent to previous experimental observations (Sharpe and Wu, 1978; Meidner and Bannister, 1979; Mott et al., 1997; Marenco et al., 2006; Mott and Peak, 2006), the dynamical model of the stomatal aperture also has abundant dynamical behaviors. In Fig. 5 (a), we show the dynamics of stomatal apertures when the atmospheric water-vapor pressure receives a sudden drop (from 2.09kPa to 1.10kPa) at time $t = 0$. For different outside-xylem conductances $K_{ox} = 10$, 15, and $20\text{mmol}/(\text{m}^2\cdot\text{s}\cdot\text{MPa})$, the stomatal dynamics after the perturbation appears to be periodic oscillatory, damped oscillatory, and monotonically convergent, respectively.

An interesting phenomenon of the stomatal dynamics is the so called "Wrong Way Response" (WWR), which is widely observed in previous experiments (Sharpe and Wu, 1978; Meidner and Bannister, 1979; Mott et al., 1997; Shope and Mott, 2008; Buckley, 2019). The WWR happens when the air humidity receives a sudden drop, which increases water loss of the leaf. In this case, a naive stomatal behavior is to reduce their aperture to resist the increased water loss. However, experimental observations have demonstrated that the stom-

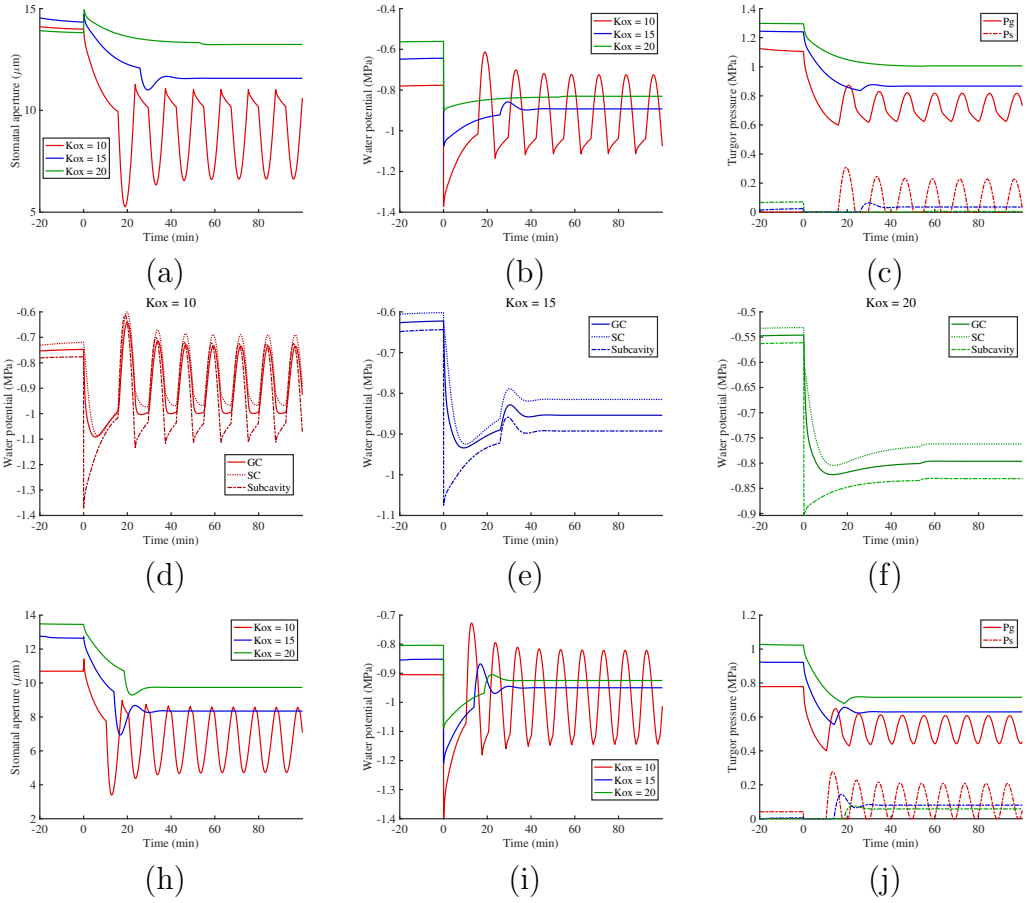

Figure 5: Stomatal dynamics. The red, blue, and green lines are used to represent simulation results obtained for outside-xylem conductance K_{ox} =10, 15, and 20mmol/m^2·s·MPa, respectively. The water-vapor pressure is decreased from $2.09kPa$ to $1.10kPa$ at time $t = 0$. (a-f) Stomatal dynamics obtained with $\Psi_x = -0.35$MPa. (a-c) Evolution of the stomatal aperture, water potential in the air cavity, and turgor pressures in the guard cells and subsidiary cells. (d-f) Evolution of the water potential in the substomatal cavity (subcavity), the guard cells (GC), and the subsidiary cells (SC) for different outside-xylem conductances. (h-j) Stomatal dynamics obtained with $\Psi_x = -0.6$MPa.

atal aperture transiently increases to a maximal size (the wrong-way response) soon after the sudden drop of air humidity, followed by a continuous decrease of aperture to be smaller than the initial value (the right-way response). As shown in Fig. 5 (a), the WWR is also observed in our simulations.

So why there is a WWR? From Fig. 5 (d-f), we can see that the difference of water potential between the the guard cells and the subsidiary cells is not significant. Therefore, we can still use the relation in Fig. 3 to understand the stomatal behavior: Before the sudden perturbation, the water potentials in the guard cells and the subsidiary cells are greater than the maximal-aperture water potential Ψ^*. After the perturbation, the water potential in the air cavity decreases quickly, which leads to a decrease of the water potential in the guard cells and the subsidiary cells. As a consequence, the stomatal aperture increases until the water potential in cells approaches Ψ^*. As the water potential decreases further, the stomatal aperture begins to decrease. Note that we have ignored the regulation process since it is much slower. From this point of view, if the atmospheric humidity is not dropped significantly, the final stomatal aperture after the perturbation can even be greater than the initial aperture. This can be verified by future experimental studies.

Note that the drop of water potential from the xylem ends to the substomatal cavity decreases with the increase of the outside-xylem conductance K_{ox}. As a consequence, the water potential in the substomatal cavity is relatively high for large K_{ox} (as shown in Fig. 5 (b)). Before the perturbation ($t < 0$), the water potential in the substomatal cavity is greater than Ψ^*. As a result, the system with smallest K_{ox} maintains the greatest stomatal aperture (as shown in Fig. 5 (a)); whereas after the perturbation, the water potential in the substomatal cavity drops to be less than Ψ^*. Then, the system with smallest K_{ox} maintains the smallest (averaged) stomatal aperture.

In our model, the oscillation frequency is mainly determined by the time scale τ for potassium transport between the guard cells and the subsidiary cells. This time scale is much greater than that for the evaporation processes. When water potential in the guard cells drops, potassium ions move from the guard cells to the subsidiary cells. This lead to an increase of subsidiary-cell turgor and a decrease of guard-cell turgor (as shown in Fig. 5 (c)), which results in contraction of stomatal aperture. Then, the stomatal contraction increases the water potential in the air cavity, which is followed by an opposite movement of the stomatal dynamics. As a consequence, the dynamics becomes oscillatory. When the change of water potential is not large enough, potassium movement is not significant. In this case, the change of turgor pressure in the subsidiary cells is insignificant and the dynamics becomes damped oscillatory or even overdamped.

In Fig. 5 (h-j), the stomatal dynamics is obtained with a lower water potential at the xylem end, $\Psi_x = -0.6$MPa, which means poor water supply of the leaf. A major difference in the dynamics is the disappearance of the WWR. This is mainly because the initial water potential in the substomatal cavity (and the stomatal cells) is already less than the maximal-aperture water potential Ψ^*.

4.2. Steady state relations

In real applications, one may be interested in predicting the change of stomatal aperture and transpiration rate when environmental conditions are changed. Such relations may be used to study the environment adaptability of a plant specie or optimize the irrigation strategy.

Once all the physical parameters are carefully measured, our model can be used to obtain such relations. For simplicity, we use the steady-state dynamics to obtain such relations, though there are numerical errors when the system becomes oscillatory (in this case, the proper approach is to average the aperture or transpiration rate over one period). Note that these relations are obtained for natural environment and the water potential in the substomatal cavity is not determined a priori. This is different from that shown in Fig. 3, in which the leaf is soaked in a solution with a given water potential.

In Fig. 6, we show the stomatal apertures and transpiration rates evaluated for different atmosphere water potential. As we increase the atmosphere humidity, the stomatal aperture increases and reaches the maximum at a certain atmosphere vapor pressure. Further increase of the air humidity leads to reduction of stomatal aperture.

Not surprisingly, the transpiration rate decreases with the air humidity. The slope of the transpiration rate is relatively small when the air is dry, showing a buffering effect of the transpiration to environmental changes. This is helpful for plants to save water in dry air environment. As shown in Fig. 6 (a-b), the influence of wind speed v_{wind} is not significant. Nevertheless, this influence can become significant for leaves with a larger radius A_r. This is related to the ratio between the two terms in the boundary layer resistance defined in Eq. (10). Meanwhile, as shown in Fig. 6 (c-d), the outside-xylem conductance plays an important role in these relations.

In Fig. 7, we show the stomatal apertures and the transpiration rates evaluated for different water potential at the xylem end. This can be used to understand the stomatal behavior under different water supply of the leaf. As shown in Fig. 7 (a-b), when the atmosphere is relatively dry, better water supply (high water potential Ψ_x) corresponds to larger stomatal apertures and larger evaporation rates. Nevertheless, when the atmosphere is humid (e.g., $e_{air} = 2.2kPa$MPa), sufficiently low xylem water potential Ψ_x is helpful for

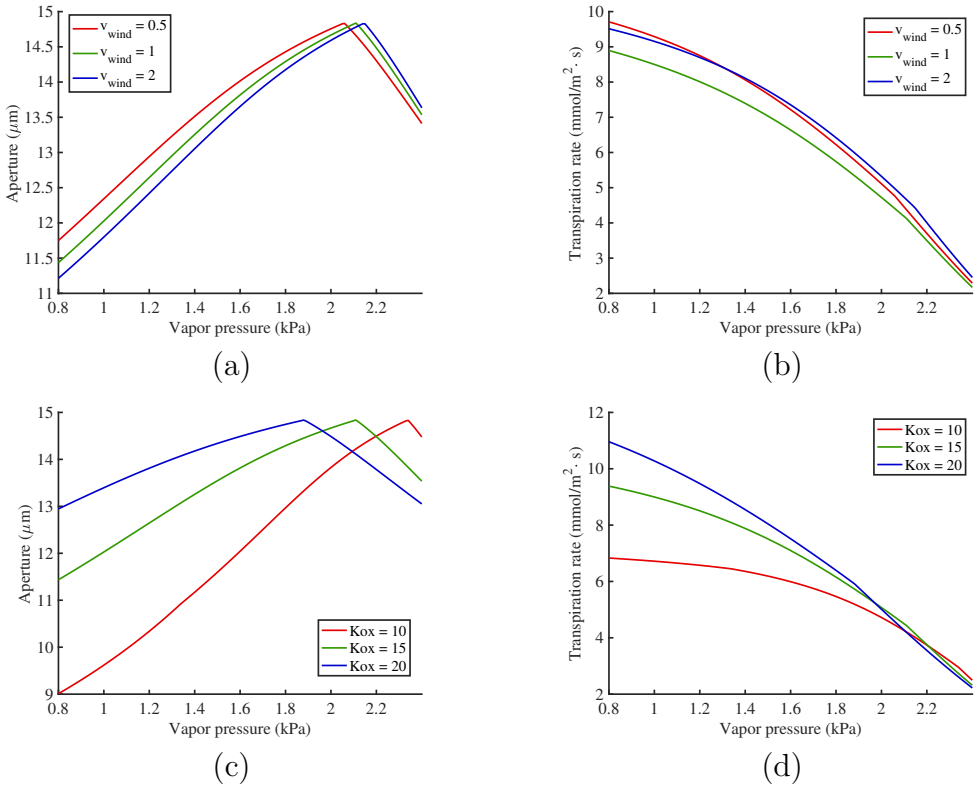

Figure 6: Stomatal apertures and transpiration rates evaluated for different atmosphere water potential. (a-b) Results obtained with $\Psi_x = -0.35$MPa, $Kox = 15$mmol/MPa·m^2·s, and different wind speed. (c-d) Results obtained with $\Psi_x = -0.35$MPa, $v_{wind} = 1$m/s, and different outside-xylem conductances.

the leaf to maintain large stomatal apertures and enhance the acquisition of carbon-dioxide. Again, as shown in Fig. 7 (c-d), the outside-xylem conductance influence the results significantly.

5. Model comparison

Due to the importance of the stoma, there have been many different models for the stomatal behavior. Nice reviews of these models can be found in previous works (Damour et al., 2010; Buckley and Mott, 2013). Here we briefly compare our model with a few representative previous models.

Our model is a mechanical model for the stomatal complex, in which the stomatal conductances and apertures are physically determined. This is different from empirical models for the stomata conductances, such as the Ball-Berry model (Ball and Berry, 1987) and variations thereof (Leuning, 1990, 1995), which are usually combined with a separate model for the stomatal aperture (Buckley and Farquhar, 2003). In our steady-state model, the determination of stomatal conductance and the stomatal aperture are coupled with each other. Although our dynamical model are more complicated than empirical or semi-empirical models, it can also be more powerful in predicting stomata responses to different environment conditions.

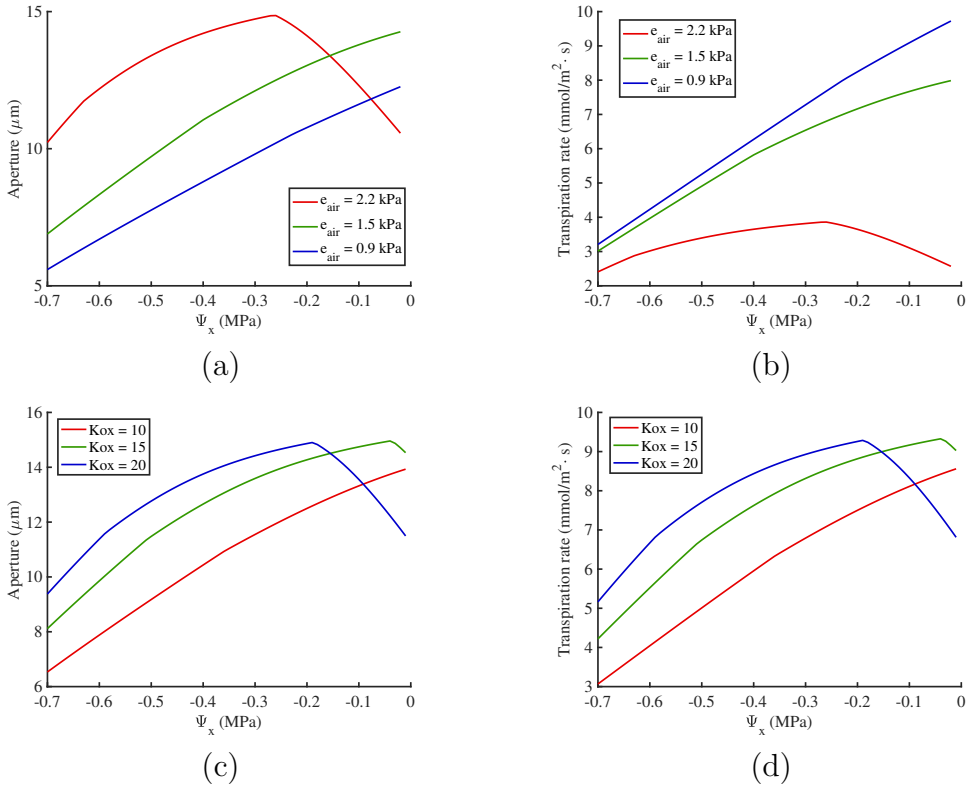

Figure 7: Stomatal apertures and transpiration rates evaluated for different water potential at xylem ends. (a-b) Results obtained with $Kox = 10\text{mmol/MPa}\cdot\text{m}^2\cdot\text{s}$, and different air humidity. (c-d) Results obtained with $e_{air} = 1.37kPa$, and different outside-xylem conductances. The wind speed is set to be $v_{wind} = 1\text{m/s}$.

The framework of our mechanical model is similar to a few previous mechanical models (Delwiche and Cooke, 1977; Dewar, 2002; Kwon and Choi, 2014). Compared to these models, the stomatal aperture is determined by the elastic interaction between guard cells and subsidiary cells in our model. As a consequence, the bivariate function $a = a(P_g, P_s)$ is used to determine the stomatal aperture based on experimental data. Compared to the model in Ref. (Delwiche and Cooke, 1977), we have incorporated the active control of potassium flux in our model. The active control model for solute movement in Refs. (Dewar, 2002; Kwon and Choi, 2014) has similar effects with our model, though they are formulated by the osmotic pressure. Different to our model, plasmolysis (zero turgor pressure) of cells is not allowed in Refs. (Kwon and Choi, 2014), which is inconsistent with experimental observations (Franks and Farquhar, 2007). In Ref. (Dewar, 2002), the difference of water potential between guard cells and epidermal cells are directly used to determine the transpiration rate, whereas in our model, the transpiration rate is physically determined by the stomatal aperture (coupled model) and the vapor pressure difference between the substomatal cavity and the atmosphere. The model in Ref. (Kwon and Choi, 2014) assumes a slow relaxation of evaporation rate of guard cells and mesophyll cells to the evaporation rate, which should be a fast

process compared with the active regulation of cell solutes.

The improvements in our model allows us to explain more experimental phenomena, such as Glinka's experiment and the Wrong-way response of stomata. Similar to previous models, our model is capable of predicting transpiration rate and stomatal conductances on the whole-leaf level. Meanwhile, our model is particularly suitable to describe the dynamics of single stomata, which can be further utilized to explain the collective dynamics of stomata such as stomatal patchiness (Cardon et al., 1994).

6. Discussions and conclusions

In this work, we develop a mathematical model for the stomatal behavior of seed plants. Despite the diversity in geometry and configuration of the stomatal complex among plant species, we use a two-element model of the guard cells and the subsidiary cells to describe the stomatal behavior. Based on existing experimental results and simple assumptions, we develop the passive mechanical model and the active control model.

Using our stomata model, we have made successful predictions to explain different experimental observations, including Glinka's results (Glinka, 1971) and the wrong-way response (Sharpe and Wu, 1978; Meidner and Bannister, 1979; Mott et al., 1997; Shope and Mott, 2008; Buckley, 2019). Consistent with the experimental observations, our model of stomatal aperture contains rich dynamical behavior. In particular, the oscillatory dynamics provides further possibility to explain stomatal patchiness (Marenco et al., 2006; Mott and Peak, 2006). These successes and consistence validate our model qualitatively, though many parameters for a particular plant specie should be measured independently.

The particular geometry and configuration of the stomatal complex may be important for the adaptability of plant species. Nevertheless, we believe that their major function is similar. The subsidiary cells (or neighboring epidermal cells in a few species) play as both a mechanical support and a potassium reservoir. The details of the geometry and configuration may only contribute to tuning the bivariate function $a(P_g, P_s)$.

Although there are a lot of parameters in our model, many of them have a clear physical meaning and can be directly measured by experiments; Other parameters are only used to describe the two functions — the bivariate function $a(P_g, P_s)$ of the passive mechanical model and the target relation between the potassium ion content and the water potential of guard cells $I_g^K(\Psi_g)$ — which can be directly fitted from independent experimental data. In this work, we have utilized experimental results of different species to obtain the parameters. Nevertheless, experimental data are still insufficient to determine all the

parameters, though it is possible to estimate the magnitude of many physical parameters. We have used rather simple functions to describe the passive mechanical model and the target relation of active regulation. From this point of view, the predictions of our model are still meaningful. Further development of experimental techniques are of particular importance in measuring all the parameters and improvement of our model.

Once all the parameters in our model are determined for a particular specie, the model is powerful in predicting the stomatal behavior and the transpiration rate under different environmental conditions. Such predictions may be important in explaining plant adaptability under climate change. It may also provide useful knowledge for agricultural irrigation. As suggested by our model, when the atmosphere is very humid, our model suggests that the soil should be kept sufficiently dry to avoid stomatal close due to high water potential in the leaf. In principle, the irrigation strategy can be optimized based on our model.

Due to lack of experimental results, we have not incorporate the response the stomata to a few important environmental conditions, including light intensity and carbon-dioxide concentration. These factors are likely to affect the target potassium content in guard cells under different water potential. With corresponding experimental data, we can include such effects into our model naturally.

Acknowledgement

This work is supported by the National Key R&D Program of China (2019YFA0709503), the National Natural Science Foundation of China (Contract no. 11971312), and Student Innovation Center, Shanghai Jiao Tong University.

References

Andres, Z., Perez-Hormaeche, J., Leidi, E.O., Schlucking, K., Steinhorst, L., Mclachlan, D.H., Schumacher, K., Hetherington, A.M., Kudla, J., Cubero, B.a., 2014. Control of vacuolar dynamics and regulation of stomatal aperture by tonoplast potassium uptake. Proceedings of the National Academy of Sciences of the United States of America 111, E1806.

Ball, J. T., W.I.E., Berry, J.A., 1987. A model predicting stomatal conductance and its contribution to the control of photosynthesis under different environmental conditions. Progress in photosynthesis research , 221–224.

Blatt, M.R., 2000. Cellular signaling and volume control in stomatal movements in plants. Annual Review of Cell and Developmental Biology 16, 221.

562 Brodribb, T.J., McAdam, S. A., J.G.J.M.S.C., 2014. Conifer species adapt to
563 low-rainfall climates by following one of two divergent pathways. Proceedings
564 of the National Academy of Sciences of the United States of America .

565 Brodribb, T.J., McAdam, S.A., 2011. Passive origins of stomatal control in
566 vascular plants. Science 331, 582–585.

567 Brodribb, T.J., McAdam, S.A., Murphy, M.C., 2016. Xylem and stomata,
568 coordinated through time and space. Plant, Cell & Environment .

569 Buckley, T. N., M.K.A., Farquhar, G.D., 2003. A hydromechanical and bio-
570 chemical model of stomatal conductance. Plant, Cell & Environment 26,
571 1767–1785.

572 Buckley, T.N., 2016. Stomatal responses to humidity: has the black box finally
573 been opened? Plant Cell & Environment .

574 Buckley, T.N., 2019. How do stomata respond to water status? New Phytol-
575 ogist 224.

576 Buckley, T.N., Mott, K.A., 2013. Modeling stomatal conductance in response
577 to environmental factors. Plant Cell & Environment 36.

578 Cardon, Z.G., Mott, K.A., Berry, J.A., 1994. Dynamics of patchy stomatal
579 movements, and their contribution to steady state and oscillating stomatal
580 conductance calculated using gas exchange techniques. Plant Cell & Envi-
581 ronment 17, 995–1007.

582 Cooke, J.R., De Baerdemaeker, J.G., Rand, R.H., Mang, H.A., 1976. A finite
583 element shell analysis of guard cell deformations. Transactions of the ASAE
584 19, 1107–1121.

585 Damour, G., Simonneau, T., Cochard, H., Urban, L., 2010. An overview of
586 models of stomatal conductance at the leaf level. Plant Cell & Environment
587 33, 1419–1438.

588 Delwiche, M.J., Cooke, J.R., 1977. An analytical model of the hydraulic as-
589 pects of stomatal dynamics. Journal of theoretical biology, 69(1), 113-141.
590 69, 113–141.

591 Dewar, R., 2002. The ball berry leuning and tardieu davies stomatal models:
592 synthesis and extension within a spatially aggregated picture of guard cell
593 function. Plant, Cell & Environment 25, 1383–1398.

594 Dow, G.J., Bergmann, D.C., Berry, J.A., 2014. An integrated model of stom-
595 atal development and leaf physiology. New Phytologist 201.

Franks, P.J., C.I.T.S.C.A.L.J.F.G., 1995. Guard cell pressure/aperture characteristics measured with the pressure probe. Plant, Cell & Environment 18, 795–800.

Franks, P., I.R., C., G.D., F., 1998. A study of stomatal mechanics using the cell pressure probe. Plant, Cell & Environment 21, 94–100.

Franks, P.J., Farquhar, G.D., 2007. The mechanical diversity of stomata and its significance in gas exchange control. Plant physiology 143, 78–87.

G, D, Humble, K, Raschke, 1971. Stomatal opening quantitatively related to potassium transport: evidence from electron probe analysis. Plant physiology .

Glinka, Z., 1971. The effect of epidermal cell water potential on stomatal response to illumination of leaf discs of vicia faba. Physiologia plantarum 24, 476–479.

Gray, A., Liu, L., Facette, M., 2020. Flanking support: How subsidiary cells contribute to stomatal form and function. Frontiers in Plant Science 11, 881.

Hedrich, R.R., 2005. In the light of stomatal opening: new insights into the watergate. New Phytologist 167, 665–691.

Hetherington, A.M., Woodward, F.I., 2003. The role of stomata in sensing and driving environmental change. Nature 424, 901–908.

Inoue, S.I., Kinoshita, T., 2017. Blue light regulation of stomatal opening and the plasma membrane hatpase. Plant Physiology , 531.

Katelyn, H., McKown, Dominique, C., Bergmann, 2018. Grass stomata. Current biology .

Katul, G., Manzoni, S., Palmroth, S., 2010. A stomatal optimization theory to describe the effects of atmospheric co2 on leaf photosynthesis and transpiration. Annals of Botany 105, 431–442.

Kelly, Anne E., G.M.L., 2008. Rapid shifts in plant distribution with recent climate change. Proc Nat Acad Sci Usa .

Kollist, H., Nuhkat, M., Roelfsema, M., 2014. Closing gaps: linking elements that control stomatal movement. New Phytologist 203.

Kwon, H.W., Choi, M.Y., 2014. Generalized hydromechanical model for stomatal responses to hydraulic perturbations. Journal of Theoretical Biology , 119–130.

Lawson, T., Blatt, M.R., 2014. Stomatal size, speed, and responsiveness impact on photosynthesis and water use efficiency. PLANT PHYSIOLOGY 164, 1556–1570.

Leuning, R., 1990. Modeling stomatal behavior and and photosynthesis of eucalyptus grandis. Functional Plant Biology 17, 159–175.

Leuning, R., 1995. A critical appraisal of a combined stomatal-photosynthesis model for c3 plants. Plant, Cell & Environment 18, 339–355.

Macarisin, D., Bauchan, G., Fayer, R., 2010. Spinacia oleracea l. leaf stomata harboring cryptosporidium parvum oocysts: a potential threat to food safety. Applied & Environmental Microbiology 76, 555–559.

Macrobbie, E., Lettau, J., 1980. Potassium content and aperture in "intact" stomatal and epidermal cells of commelina communis l. Journal of Membrane Biology 56, 249–256.

Marenco, R.A., Katharina, S., D., F.G., C., B.M., 2006. Hydraulically based stomatal oscillations and stomatal patchiness in gossypium hirsutum. Functional Plant Biology 33, 1103.

Martin Venturas D., Sperry, J.S., Hacke, U.G., 2017. Plant xylem hydraulics:what we understand,current research,and future challenges. Journal of Integrative Plant Biology 06, 10–43.

Meidner, H., Bannister, P., 1979. Pressure and solute potentials in stomatal cells of tradescantia virginiana. Journal of Experimental Botany , 255–265.

Miner, G.L., Bauerle, W.L., Baldocchi, D.D., 2017. Estimating the sensitivity of stomatal conductance to photosynthesis: a review. Plant Cell & Environment .

Mott, K.A., Buckley, T.N., 1998. Stomatal heterogeneity. Journal of Experimental Botany 49, 407–417.

Mott, K.A., Buckley, T.N., 2000. Patchy stomatal conductance: emergent collective behaviour of stomata. Trends in plant science .

Mott, K.A., Cardon, Z.G., Berry, J.A., 1993. Asymmetric patchy stomatal closure for the two surfaces of xanthium strumarium l. leaves at low humidity. Plant, Cell & Environment 16.

Mott, K.A., Denne, F., Powell, J., 1997. Interactions among stomata in response to perturbations in humidity. Plant, Cell & Environment 20, 1098–1107.

Mott, K.A., Peak, D., 2006. Stomatal patchiness and taskperforming networks. Annals of Botany 99.

Mott, K.A., Sibbernsen, E.D., Shope, J.C., 2008. The role of the mesophyll in stomatal responses to light and co 2. Plant Cell & Environment 552, 203–207.

PETER, J.H., HSIN-I, S., WU, 1978. Stomatal mechanics: volume changes during opening. Plant, Cell & Environment 1, 259–268.

Raschke, K., Hedrich, R., Reckmann, U., Schroeder, J.I., 1988. Exploring biophysical and biochemical components of the osmotic motor that drives stomatal movement. Plant Biology 101, 283–294.

Rockwell, F.E., Holbrook, N.M., Stroock, A.D., 2014. The competition between liquid and vapor transport in transpiring leaves (1[w][open]). Plant physiology .

Sack, L., Holbrook, N.M., 2006. Leaf hydraulics. Annual Review of Plant Biology .

Scoffoni, C., Albuquerque, C., Brodersen, C.R., Townes, S.V., John, G.P., Bartlett, M.K., Buckley, T.N., Mcelrone, A.J., Sack, L., 2017. Outside-xylem vulnerability, not xylem embolism, controls leaf hydraulic decline during dehydration. Plant Physiology 173, 1197–1210.

Shahraeeni, E., P., L., D., O., 2012. Coupling of evaporative fluxes from drying porous surfaces with air boundary layer: Characteristics of evaporation from discrete pores. Water Resources Research 48, 9525.

Sharpe, P.J., Wu, H., 1978. Stomatal mechanics: volume changes during opening. Plant, Cell and Environment 1, 259–268.

Shope, J. C., P.D., Mott, K.A., 2008. Stomatal responses to humidity in isolated epidermes. Plant, Cell & Environment 31, 1290–1298.

Steudle, E., Zimmermann, U., Luttge, U., 1977. Effect of turgor pressure and cell size on the wall elasticity of plant cells. Plant Physiology 59, 285–289.

Vesala, T., 1998. On the concept of leaf boundary layer resistance for forced convection. Journal of Theoretical Biology 194, 91–100.

Zimmermann, U., Schulze, H.D., 1980. Direct turgor pressure measurements in individual leaf cells of tradescantia virginiana. Planta 149, 445–453.

Appendices

Since the diffusion process of water molecules is much faster than the stomatal dynamics, we assume that the diffusion process always reaches at steady states. Thus the transpiration flux can be estimated by (in the unit of mmol/m^2·s)

$$K_{ox}(\Psi_x - \Psi_2) = \frac{e_2 - e_{air}}{RT(R_{st} + R_{bl})}, \tag{13}$$

where the left hand side is the water flux from xylem ends to the substomatal cavity and the right hand side is the water flux from substomatal cavity to the atmosphere. Using the Taylor expansion of Eq. (11), we have

$$K_{ox}(\Psi_x - \Psi_2) \approx K_{ox}\frac{RT}{V_m}\frac{e_x - e_2}{e_w} = \frac{e_2 - e_{air}}{RT(R_{st} + R_{bl})}. \tag{14}$$

By define $R_{ox} = \frac{V_m e_w}{(RT)^2}\frac{1}{K_{ox}}$, we obtain

$$e_2 = \gamma(a)e_x + (1 - \gamma(a))e_{air}, \tag{15}$$

where

$$\gamma(a) = \frac{R_{ox}}{R_{ox} + R_{st}(a) + R_{bl}(a)}. \tag{16}$$

Typically, $\gamma(a)$ is only a few thousandths in magnitude.